A reverse-time migration workflow of passive source with joint imaging conditions

Bin Lyu, Nori Nakata, and Kurt J. Marfurt, The University of Oklahoma*

SUMMARY

Passive-source reverse-time migration (PS-RTM) is an effective tool for imaging complex seismic discontinuities and scatters for both regional and global problems. It is generally implemented by first back propagating the multicomponent seismic recordings, then followed by a cross-correlation imaging condition. However, it faces the challenges of data components requirement, wave mode separation, and velocity updating. We present a PS-RTM workflow by using joint imaging conditions. First, we use a geometric-mean RTM method to locate the passive seismic sources. Then we perform the RTM imaging with a squared excitation amplitude imaging condition, to provide high-resolution seismic images. We evaluate the workflow with a synthetic horizontal-reflector model and a part of the Marmousi model.

INTRODUCTION

Seismic imaging of passive sources provides crucial subsurface information. Common conversion points (CCP) method has been widely used to image the subsurface velocity discontinuity interfaces. It is realized by stacking the receiver functions at the CCP. However, CCP method could not handle the imaging of complex structures, because it does not account for the effects of wave diffraction and scattering caused by the lateral variations in the interfaces. Shang et al. (2012) use a passive-source reverse-time migration (PS-RTM) method to improve the imaging precision by using the converted waves. PS-RTM is implemented first by back propagating the recorded multicomponent seismic data. Then the P and S wave fields will be separated by polarization decomposition for each snapshot. Finally, a cross-correlation imaging condition between P and S wave components is performed to provide the seismic images. Actually, this cross-correlation imaging condition is the same with the one used by Artman et al. (2010).

In PS-RTM, only the receiver-side multicomponent wavefields are used, which is different with the active-source RTM, by using both the source-side and receiver-side wavefields. No detailed knowledge of the sources is needed in PS-RTM. It still faces several challenges. First, we need multicomponent seismic recordings to perform P and S wavefields cross-correlation. Second, accurate wave mode separation still remains challenges. Finally, extended imaging condition (Witten and Shragge, 2015) is needed for passive source velocity inversion, which introduces huge computation cost.

In our study, we developed a RTM workflow of passive source with joint imaging conditions. We first estimate the passive source locations with a geometric-mean RTM (Nakata and Beroza, 2016) method. Then we borrow the idea of active-source RTM, to provide the seismic images by using a high-resolution squared excitation amplitude imaging condition (Lyu et al., 2017). In this workflow, we can perform PS-RTM with only acoustic wavefield, which also avoids the wave mode separation. Additionally, the migrated gathers could be directly used for velocity updating. We begin with this introduction, and then followed by a detailed illustration of the workflow. We also show the numerical results of a synthetic horizontal-reflector model and a part of the Marmousi model.

METHOD

We combine two different imaging conditions to realize a RTM workflow of passive sources. It is implemented with primary 2 steps. With the passive source recordings, and an initial smoothed velocity model derived from tomography or other methods, we first estimate the source locations with a geometric-mean RTM method. Then we preform the RTM imaging with a squared excitation amplitude imaging condition with the inputs of the passive source recordings, the same smoothed velocity model, and the estimated source information from step 1. We can update the velocity model directly using the migrated gathers. With the updated velocity model, we can repeat the source estimation and RTM imaging steps, which provides an iterative workflow for both passive source estimation and velocity inversion. In this paper, we suppose that the velocity model is accurate enough and we focus on the two primary steps within one iteration.

1) Source location estimation with the geometric-mean RTM

For time-reversal imaging (TRI) (Gajewski and Tessmer 2005; Fink, 2006; Zhu, 2014), we need to perform scanning on a 4D image volume produced by the reverse-time propagation of receiver wavefields (McMechan, 1982), to estimate the source location. Several approaches are developed to reduce the dimension, such as the geometric-mean RTM (GmRTM) method, and least-squares time-reversal imaging method (Sun et al., 2016). Here, we use the GmRTM method (Nakata and Beroza, 2016) to estimate the passive source location. It is realized by performing a zero-lag cross-correlation among all the independently back-propagated receiver wavefields,

$$\mathrm{I}(\mathbf{x},t)=\prod_{i=0}^{N-1} p_i(\mathbf{x},t) \qquad (1)$$

where p_i indicates the back-propagated wavefields of different receivers. With this GmRTM, we can collapse the time axis, which reduces one dimension in the conventional TRI method. The passive sources estimated with equation 1 will be used in the next step.

2) RTM imaging with the squared excitation amplitude imaging condition

With the estimated passive source locations in step 1, we perform RTM imaging with a similar idea of active source. The seismic recordings and velocity model are the same with step 1. There are several different imaging conditions in active source RTM, such as the amplitude ratio, zero-lag cross-correlation, source-normalized cross-correlation, excitation time, and excitation amplitude. In our study, we use a squared excitation amplitude imaging condition (Lyu et al., 2017), to provide high-resolution RTM images,

$$\mathrm{I}_{\mathrm{ex}}(\mathbf{x})=\frac{\left|p_r(t_i,\mathbf{x})\right| p_r(t_i,\mathbf{x})\,\delta(t_e,\mathbf{x})}{p_{s\_\max}(t_e,\mathbf{x})\,p_{s\_\max}(t_e,\mathbf{x})} \qquad (2)$$

where t_e denotes the excitation time, and $p_{s\_\max}$ is the excitation amplitude. Actually, the squared excitation amplitude imaging condition a variation of the amplitude ratio one. We only need to save the excitation time and excitation amplitude during wave propagation, which sidesteps the large storage requirement in the cross-correlation RTM. We implement a polarization-preserved zero-lag autocorrelation on the extrapolated receiver wavefields, and the followed imaging is only implemented at the locations where satisfy the excitation time, which improves the resolution and reduces the migration artifacts.

EXAMPLES

We perform numerical tests on a synthetic horizontal-reflector model and a part of the Marmousi model, by using the presented workflow.

Horizontal-reflector model

The velocity model is shown in Figure 1a, with three horizontal reflectors. We set 5 sources (red dots) at depth 3km, with horizontal interval 100m. A smoothed version of the velocity model (Figure 1b) is used for imaging, as in real world we generally couldn't get the exact velocity model. Figure 2 shows the GmRTM result, which provides consistent source locations with our settings. We then perform the RTM imaging with squared excitation amplitude imaging condition after source location estimation. In Figure 3a and 3b, we show the excitation time and excitation amplitude of one shot. We only show the depth ranging from 0m to 2000m for comparison. Figure 4b is the stacked RTM images of these 5 passive sources using the squared excitation amplitude imaging condition, which behaves higher resolution and fewer migration artifacts over the result by cross-correlation (Figure 4a).

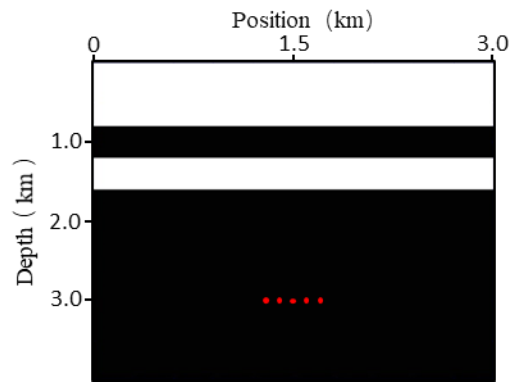

(a) True velocity model and source locations

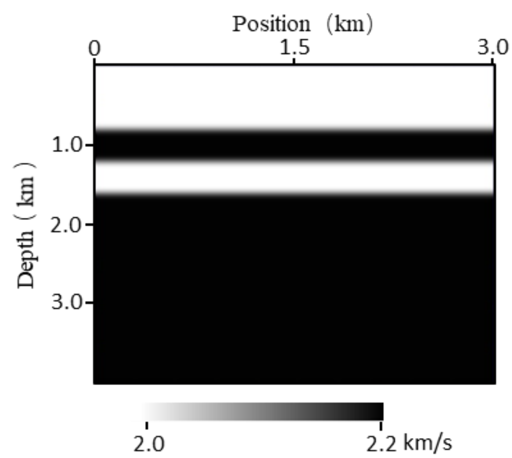

(b) Smoothed velocity model

Figure 1: Horizontal-reflector velocity model (a), and its smoothed version (b). Five passive sources are indicated by the red dots.

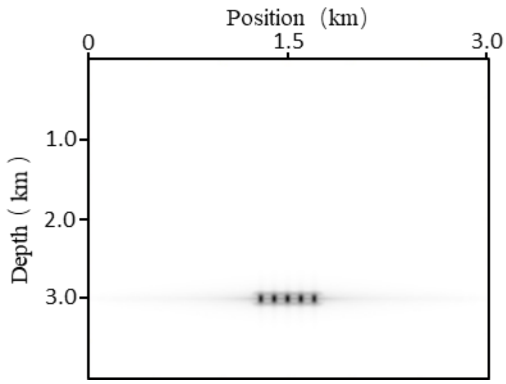

Figure 2: GmRTM result of the passive sources

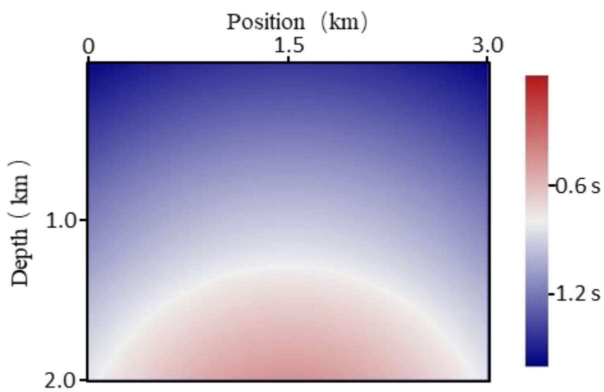

(a) Excitation time

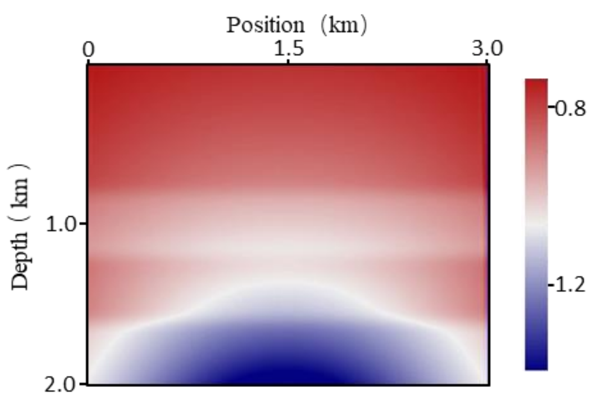

(b) Excitation amplitude

Figure 3: Excitation time (a) and excitation amplitude (b) of one source, which are used for RTM imaging.

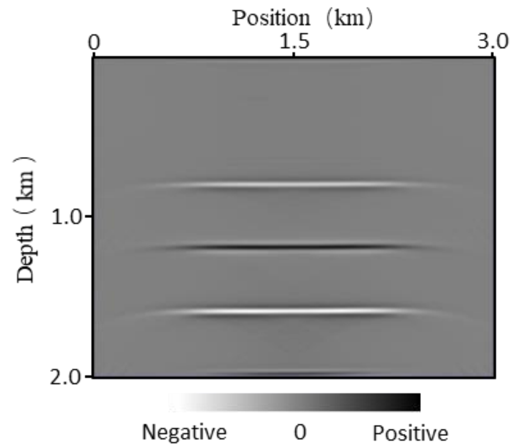

(a) Cross-correlation

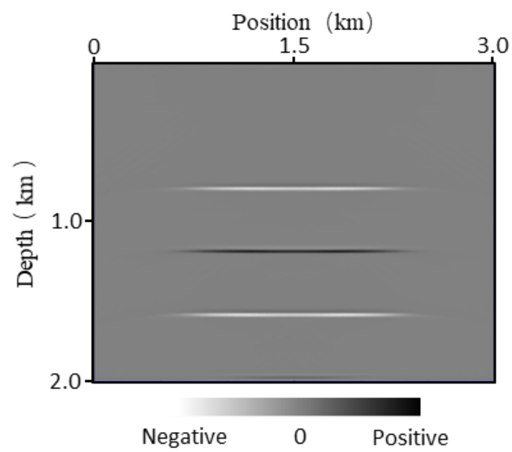

(b) Squared excitation amplitude

Figure 4: RTM images with (a) cross-correlation, and (b) squared excitation amplitude imaging conditions.

We also show the shot-domain migrated gathers with -10% velocity error (Figure 5b), and +10% velocity error (Figure 5c). Compared with the gather with correct velocity (Figure 5a), the gather with lower velocity (Figure 5b) behaves deeper and downward curves, while the one with higher velocity (Figure 5c) behaves shallower and upward curves. These observations provide a potential way for direct velocity updating. It is also noted that these observations of passive sources are different with the ones of active sources. Further research is needed to find the relation between the velocity update and the residual moveout from the migrated gathers of passive sources.

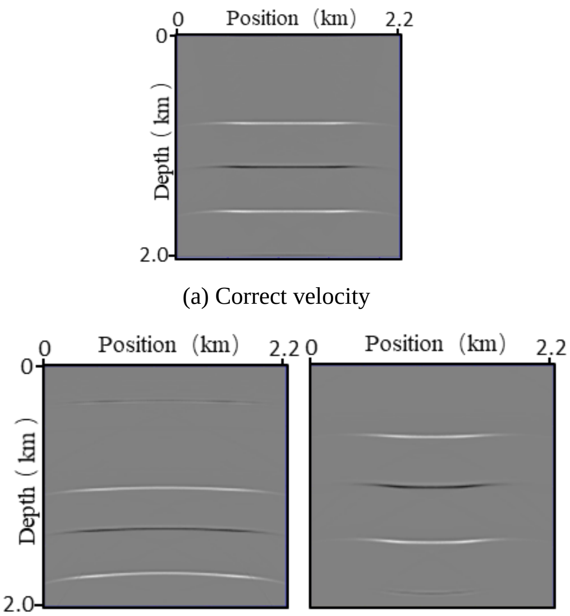

(a) Correct velocity

(b) Lower velocity (c) Higher velocity

Figure 5: Shot-domain migrated gather with (a) correct velocity, (b) velocity with -10% error, and (c) velocity with +10% error.

Marmousi model

We also perform a numerical test on a part of the Marmousi model, which is shown in Figure 6. We set 3 sources (red dots) at depth 3km, with horizontal interval 100m. We also use a smoothed version of the true velocity for imaging. We perform the GmRTM to estimate the source locations, which is shown in Figure 7. With the estimated 3 sources, we perform RTM imaging using the squared excitation amplitude imaging condition with the same passive source recordings and the smoothed velocity model. The result of the shallow imaging is shown in Figure 8, which provides high-resolution image of the thin reflectors.

CONCLUSIONS

We present a RTM workflow of passive sources with joint imaging conditions. We first apply the GmRTM method to estimate the passive sources, then followed by a squared excitation amplitude imaging condition to provide high-resolution RTM images. We can implement the PS-RTM with only acoustic seismic data. And the migrated gathers are potentially used for direct velocity updating. We only show 2D synthetic examples in this paper, but the workflow could be naturally extended to 3D.

ACKNOWLEDGEMENTS

The authors thank Dr. Zhiguang Xue for help discussions.

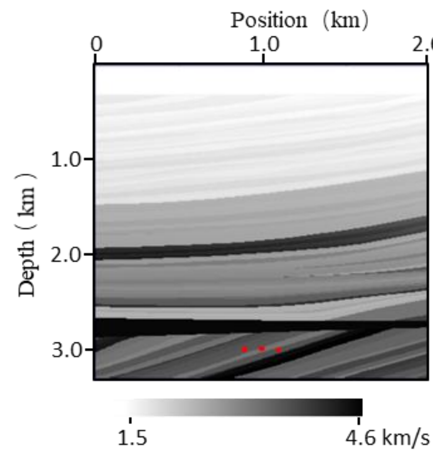

Figure 6: Part of Marmousi model with 3 passive sources

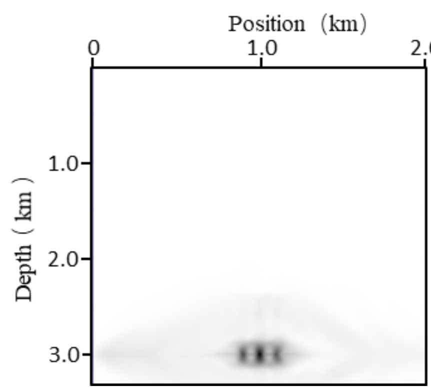

Figure 7: GmRTM result of the passive sources

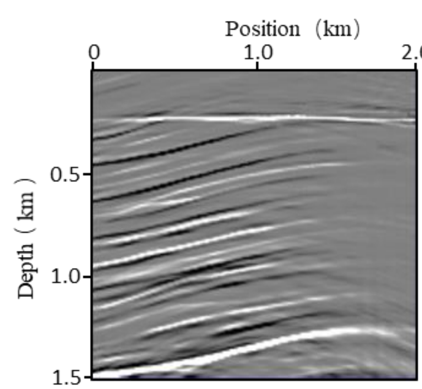

Figure 8: RTM image with squared excitation amplitude

REFERENCES

Artman, B., I. Podladtchikov, and B. Witten, 2010, Source location using time-reverse imaging: Geophysical Prospecting, 58, 861-873.

Fink, M., 2006, Time-reversal acoustics in complex environments: Geophysics, 71, no. 4, SI151-SI164.

Gajewski, D., and E. Tessmer, 2005, Reverse modelling for seismic event characterization: Geophysical Journal International, 163, 276-284.

Lyu, B., F. Li, and K. J. Marfurt, 2017, High-resolution reverse time migration with squared excitation amplitude imaging condition: SEG Expanded Abstracts, 4438-4442.

McMechan, G. A., 1982, Determination of source parameters by wavefield extrapolation: Geophysical Journal of the Royal Astronomical Society, 71, 613-628.

Nakata, N., and G. C. Beroza, 2016, Reverse time migration for microseismic sources using the geometric mean as an imaging condition: Geophysics, 81, no. 2, KS51-KS60.

Shang, X., M. de Hoop, and R. van der Hilst, 2012, Beyond receiver functions: Passive source reverse time migration and inverse scattering of converted waves: Geophysical Research Letters, 39, no. 15.

Sun, J., Z. Xue, T. Zhu, S. Fomel, and N. Nakata, 2016, Full-waveform inversion of passive seismic data for sources and velocities: 86th Annual International Meeting, SEG, Expanded Abstracts, 1405-1410.

Witten, B., and J. Shragge, 2015, Extended imaging conditions for passive seismic data: Geophysics, 80, no. 6, WC61-WC72.

Zhu, T., 2014, Time-reverse modelling of acoustic wave propagation in attenuating media: Geophysical Journal International, 197, 483-494.